The Effect of Mechanical Loading on the Frequency of an Oscillator Circuit

Report Contributors: Jonathan A. Ward[1,2],
Vladimir Lapin[1] and William Lee[1]

Study Group Contributors: Chris Budd[3], Mark Cooker[4],
Paul J. Dellar [5], Martin Hayes[6], Poul Hjorth[7],
Olga Korostynska[8] and Arno Mayrhofer[1]

Industry Representative: Sandra Healy[9]

---

[1]MACSI, Department of Mathematics and Statistics, University of Limerick, Ireland
[2]Report coordinator, jonathan.ward@ul.ie
[3]School of Mathematical Sciences, University of Bath, United Kingdom
[4]School of Mathematics, University of East Anglia, United Kingdom
[5]OCIAM, Mathematical Institute, University of Oxford, United Kingdom
[6]Department of Electronic and Computer Engineering, University of Limerick, Ireland
[7]Department of Mathematics, Technical University of Denmark, Denmark
[8]Microelectronic and Semiconductor Research Centre, University of Limerick, Ireland
[9]Analog Devices, Raheen Industrial Estate, Raheen, Limerick, Ireland

Abstract

We investigate the effect of mechanical strain on the frequency of an electronic oscillator embedded in an integrated circuit. This analysis is aimed at explaining a 1% inaccuracy in the oscillator frequency under test conditions prescribed by a leading supplier of semi-conductor devices. During the test the package containing the oscillator was clamped to a circuit board by mechanical pressure. By considering the nature of the oscillator we show that tensile strains of the order of 10^{-4} could explain the observations via the piezoresistance effect. Both a simple one-dimensional analysis based on the beam equation and an elastic finite element simulation show that strains of this magnitude can be generated during the test.

1   Introduction

Silicon chips, or Integrated Circuits (ICs), perform the underlying functions of most modern electronic devices. These miniature circuit boards consist of millions of electronic devices such as transistors, capacitors, resistors and diodes. During manufacturing, the components in ICs are built up and connected together in layers on the surface of a silicon substrate, known as a die, via etching, deposition and photo-lithography [1]. The die are then moulded into a plastic case, which we refer to as a package.

Chips are typically tested before being sold and may be moved mechanically between a variety of test sites. During testing, a downward force of the order of 100 N is exerted on the chip to ensure good electrical contact. A particular chip manufactured by a leading semi-conductor supplier (who we refer to simply as "the supplier"), contains an oscillator circuit whose frequency must reach a ±1% accuracy specification over a temperature range of −40 to +105°C and 100% of the chips are tested. However, the supplier observed that the loads experienced by the chip could lead to significant errors in the accuracy of the oscillator circuit, possibly due to some sort of piezo effect.

In this paper we investigate how a vertical load placed on such a chip might result in errors in the oscillator frequency. This problem was presented at the 70th European Study Group with Industry (ESGI), hosted by MACSI at the University of Limerick in 2009, funded by the Science Foundation Ireland mathematics initiative grant. In Section 2 we give a detailed description of the problem including the structure of the package, the test-rig set-up, data concerning the frequency response to loading and how the chips are "trimmed" to the required frequency. We describe in Section 3 how the key components in the oscillator circuit, namely capacitors and resistors, might affect the oscillator frequency when subjected to a vertical load. In Section 4 we discuss mechanical modelling of the elastic response of the package to loading using the beam equation and finite element elasticity calculations. Finally we summarise our results in Section 5.

2   Detailed Problem Description and Data

2.1   Package Design

Due to commercial sensitivity, details of the specific package and chip design cannot be presented in this paper. A sketch of the package is illustrated in Figure 1(a). There are two die in each package, one of which is smaller and sits on top of the larger (see Figure 1(b)). These are placed on a copper base known as the lead frame. The three layers are aligned at their centres and attached using epoxy adhesives. There are 8 contacts along each side of the base of the package that are connected to the die via small wires. The die, lead frame, contacts and connections are moulded into a plastic case.
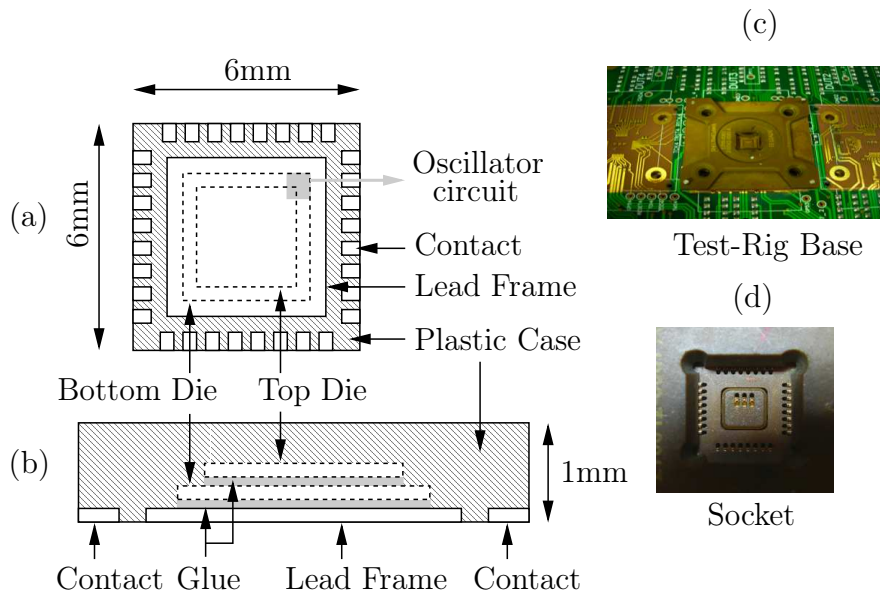
Figure 1: (a) Sketch of the base of the package (not to scale) illustrating the lead frame and contact positions. The relative positions inside the package of the top and bottom die (dashed boxes) and the oscillator circuit (shaded grey box) are indicated. (b) Cross-section of the package (larger scale than (a)). Again the positions of the lead frame, contacts and the top and bottom die are marked. The epoxy glues are also labelled. (c) Photo of the base of the test-rig in which the package is placed during testing. (d) Magnification of the socket in which the package is placed and the electrical contact pins on which it sits.

2.2   Test Rig Set-Up

During testing, each package is transported between test sites (see Figure 1(c)) using a mechanical test rig arm. This device places a small cylindrical nozzle on top of each package and then applies a suction force to attach the package to the arm before it is relocated. In each test, an individual package is placed in a plastic well on the test circuit board, where it rests on top of a set of copper pins that connect with the contacts on the base of the package (see Figure 1(d)). There are three pins positioned slightly off centre that contact the lead frame and one for each of the contacts around the edge of the package. The test rig arm exerts a vertical force on the package to ensure good electric contact, but the magnitude of this force is not known accurately and varies between different test rigs.

2.3   Problems with Frequency Response Due to Loading

As stated, the oscillator circuit in the chip must oscillate at a frequency of 128 kHz with a $\pm 1\%$ tolerance. However the supplier found that this error could not be reduced below 1.5%, which they suspected was due to the loads placed on the chip. This was confirmed using a hand test rig consisting of the standard test rig base and a locking top that applies a vertical

% Frequency Change vs. Applied Mass
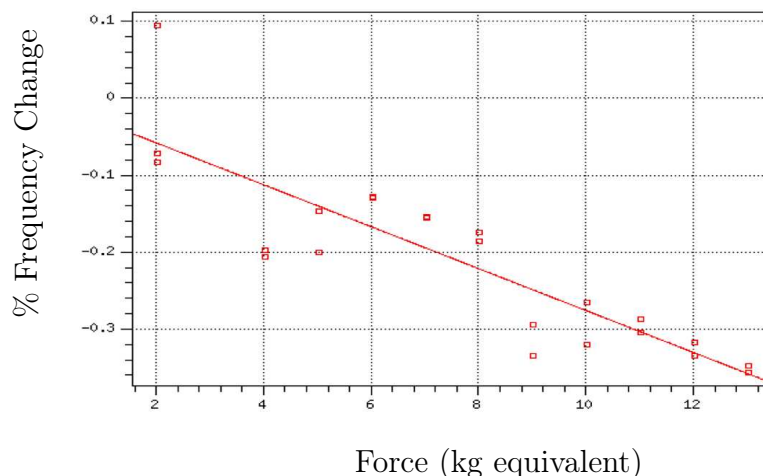
Figure 2: Data recorded by Analog Devices relating percentage change in frequency to applied mass (i.e. the load placed on top of the package). A decreasing linear response is observed. Note that a load of the order of 100 N (i.e. 10 kg) causes approximately a -0.3% error. Thus the testing process alone wastes a significant amount of the specified tolerance.

force to the chip via a hand operated screw mechanism. Although variations in frequency were observed during the hand test, the amount of force applied during the test was not quantifiable in any way. Furthermore, the hand test rig is not used during the actual testing of the chips, so is only an indication that loading of the chip affects the oscillator frequency.

To quantify the effect caused by loading the package, the supplier collected a small amount of preliminary quantitative data, illustrated in Figure 2, by applying a range of vertical loads to a given package. The results of this experiment suggest a linear relationship between the load applied and the frequency response of the oscillator circuit, although it is stressed that the data is only indicative. Note that these experiments indicate that for a load of the order of 100 N (i.e. 10 kg), a -0.3% error is observed. Thus a significant amount of the specified tolerance is wasted on the testing process alone, which must be compensated for by higher manufacturing precision.

2.4   Circuit Trimming

Banks of components (including resistors and capacitors) are used to tune the oscillator to the required frequency over the given temperature range. This process is known as trimming, and in the traditional sense would mean that particular components were removed permanently from the active circuit. In this instance, a flash memory stores the identities of the trimmed components.

3 Piezo Effects in the Oscillator Circuit

We now describe how the response of the key components in the oscillator circuit might be affected by mechanical loading. An oscillator circuit provides a continuous, synchronised trigger signal to the rest of the devices on the chip from which information is processed [2]. Due to commercial sensitivity (and its shear complexity), the specific design of the oscillator circuit in question was not provided. However, there are two main types of electronic oscillators, RC circuits (composed of *R*esistors and *C*apacitors) and LC circuits (composed of inductors and capacitors). Inductors are not common in ICs, hence we focus on the first type of oscillator.

The oscillation frequency of an RC circuit is $f = 1/(2\pi RC)$ [1], where R and C are the effective resistance and capacitance of the banks of resistors and capacitors on the chip respectively. Typical values of resistance and capacitance are $R = 10\text{k}\Omega$ and $C = 100\text{pF}$. A small fractional increase, δ, in the product of the resistance and capacitance results in a fractional decrease in frequency, f, of the same amount,

$$f = \frac{1}{2\pi RC(1 + \delta)} \approx \frac{1}{2\pi RC}(1 - \delta). \tag{3.1}$$

Thus a 1% drop in frequency requires a 1% increase in capacitance or resistance (i.e. $\delta = 0.01$). We now consider whether the kind of mechanical load experienced by the chip can give rise to such changes in the capacitance or resistance.

3.1 Capacitor Response

Capacitors consist of two parallel conducting plates with a dielectric material sandwiched between. The plane of the conducting plates is perpendicular to the applied load in this case. The value of capacitance is given by

$$C = \frac{\varepsilon A_C}{d}, \tag{3.2}$$

where ε is the permittivity of the dielectric, A_C is the area of the plates and d is the distance between them. Thus the capacitance increases in response to a decrease in distance between plates, which might be expected when subjected to a vertical load as in this scenario.

However, the dielectric material is typically silicon dioxide, which is a very stiff material. Given a 100N force placed on a package approximately 6mm×6mm, the resulting pressure P is 4 MPa. The Young's modulus E of silicon dioxide is approximately 100 GPa, thus considering Hooke's law, the resulting strain (and hence the change in distance between plates) is

$$\frac{P}{E} \simeq 3 \times 10^{-5}, \tag{3.3}$$

which is much smaller then the 1.5% change required.

Thus the change in capacitance due to the plates being forced closer together cannot be responsible for the observed 1.5% change in frequency. The deformation of the dielectric does not change its permittivity either, since silicon dioxide does exhibit any piezoelectric effects [3].

3.2 Resistor Response

Piezoresistance is a well known effect that occurs when resistors are subject to mechanical deformation [4]. The resistance of a conducting element with a fixed cross section of area A_R and length l is given by

$$R_0 = \rho_0 \frac{l}{A_R}, \tag{3.4}$$

where ρ_0 is resistivity. If the shape of the resistor is changed, the subsequent change in resistance is related to the strain $\epsilon = \Delta l / l$ via

$$\frac{\Delta R}{R_0} = G\epsilon, \tag{3.5}$$

where G is known as the gauge factor,

$$G := (1 + 2\nu) + \frac{(\Delta \rho / \rho_0)}{\epsilon}, \tag{3.6}$$

and ν is the Poisson's ratio of the resistor material, which accounts for the change in cross-sectional area due to the change in length. It is known that the resistivity change $(\Delta \rho / \rho_0)/\epsilon$ for semiconductors is much larger than the dimensional change $(1 + 2\nu)$ [5]. In fact gauge factors as large as 100 have been measured for p-type silicon and as low as -100 in n-type silicon [4, 6]. Thus to observe a 1% decrease in frequency due to piezoresistance, we would need strains of the order of 10^{-4}.

4 Mechanical Modelling

To calculate the strains induced by mechanical loading, we first consider a simple method in which the package is modelled using a one-dimensional beam equation. This approach neglects inhomogeneities in the package and corner effects that arise in the plane perpendicular to the loading due to the stacking of the die. Thus we develop a more sophisticated two-dimensional axisymmetric model of the composite package that we solve using finite element software in COMSOL, from which we obtain the strain field in a cross-section of the package.

4.1 One-Dimensional Model

A simple approach to calculating approximate values of the strain in the package is to model the entire assembly using the one-dimensional beam equation [7]. Thus we consider the package
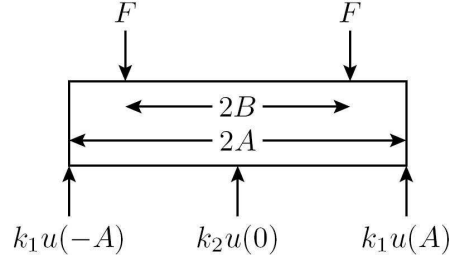
Figure 3: Geometry in which the package is modelled as an elastic beam. The pins are modelled as Hookean springs, while the die is modelled as two localised forces.

to be elastically homogeneous and made entirely of silicon. The geometry used in this case is shown in Figure 3. The width of the package is $2A$ and the load is represented by two localised forces F imposed at $x = \pm B$. The pins are modelled as Hookean springs, positioned at the edges of the package ($x = \pm A$) and the centre ($x = 0$) with spring constants k_1 and k_2 respectively. The spring constant of the outer pins is chosen to be five times larger than at the centre to reflect that there are more pins around the edge of the package. However, the spring constants are not known accurately,thus we consider two cases: (a), stiff springs, $k_1 = 500$ MN/m and $k_2 = 100$ MN/m ; and (b), flexible springs, $k_1 = 50$ MN/m and $k_2 = 10$ MN/m .

As noted, we model the vertical displacement $u(x)$ of the package using the one-dimensional beam equation with point forcing,

$$EI\frac{d^4u}{dx^4} = F\left[\delta(x + B) + \delta(x - B)\right] - k_2\delta(x)\,u(x), \tag{4.1}$$

where E is the Young's modulus of the package and I is the second moment of area. The boundary conditions at the edges of the package are

$$EI\left.\frac{d^3u}{dx^3}\right|_{x=\pm A} = -k_1u(\pm A) \quad \text{and} \tag{4.2}$$

$$\left.\frac{d^2u}{dx^2}\right|_{x=\pm A} = 0. \tag{4.3}$$

Note that at each discontinuity, the zeroth, first and second derivatives must be equal. These equations form a linear system whose solution is a piecewise cubic polynomial in x. The polynomial coefficients in each of the four regions along the beam can be easily calculated using computer algebra, however they are somewhat complicated and hence we do not reproduce them here.

The parameters used in the calculation are given in Table 1. The displacement along the beam $u(x)$ is illustrated in Figure 4(a) for the stiff springs case and in Figure 4(b) for the case flexible springs case. These illustrate that the stiffness of the pins can affect the overall shape of the package: stiffer pins result in a "W"–shape, whereas flexible pins give rise to a concave shape.

36

Parameter	Value	
A	3	mm
B	2	mm
h	1	mm
E	150	GPa
F	50	N

Table 1: Values of parameters used in the calculation. In addition, two different types of spring constant are considered: stiff springs, $k_1 = 500$ MN/m and $k_2 = 100$ MN/m ; and flexible springs, $k_1 = 50$ MN/m and $k_2 = 10$ MN/m .
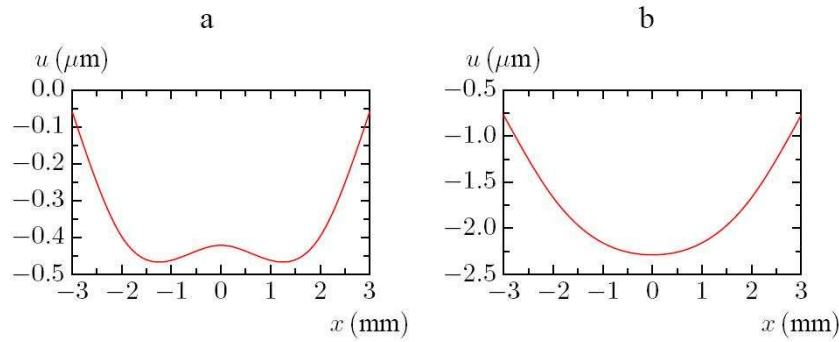
Figure 4: Displacement calculated from equations 4.1–4.3 for the cases (a) (stiff springs) and (b) (flexible springs).

Given the displacement and the height of the package h, we can calculate the tensile strain,

$$\epsilon_{xx} = \frac{h}{2}\frac{d^2 u}{dx^2},\tag{4.4}$$

at the base of the package. This is plotted in Figure 5(a) and (b) for the stiff and flexible pin cases respectively. In both instances, the magnitude of the strains are large enough to account for the observed frequency variations due to piezoresistive effects. The stiffer springs used in Figure 4(a) result in a region of compression at the centre of the package. Note that in both cases, the largest strains occur in regions of extension (positive strain) where the downward load is applied. The strain is zero at the edges due to the boundary conditions (4.3).

4.2 Axisymmetric Finite Element Model

Although the simple approach using the beam equation shows some promising results, it is based on a very restrictive set of assumptions, in particular that the package is homogeneous and can be represented as thin rod. A linear elasticity model of the composite package can be

37
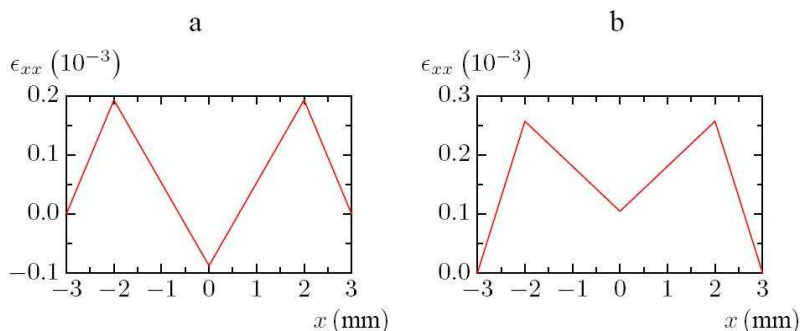
Figure 5: Tensile strain at the base of the package for cases (a) (stiff springs) and (b) (flexible springs).

computed numerically using finite element methods. To facilitate this, we used the Structural Mechanics Module of COMSOL 3.4 software package [8]. This includes a stationary linear solver for the equilibrium equation from linear elasticity theory,

$$\sigma_{ij,j} = 0$$

where $\sigma_{ij,j}$ is the derivative with respect to j of the ij component of the stress tensor. This is supplemented with the linear stress-strain and strain-displacement relationships,

$$
\begin{aligned}
\sigma_{ij} &= \lambda\epsilon_{kk}\delta_{ij} + 2\mu\epsilon_{ij}, \\
\epsilon_{ij} &= 1/2\left(u_{i,j} + u_{j,i}\right),
\end{aligned}
$$

respectively where ϵ is the strain tensor, u is the displacement and λ and μ are Lamé's parameters, which can be expressed in terms of the Poisson's ratio and Young's modulus. We used 2nd-order Lagrange finite elements with ideal constraints.

The simulation set-up is illustrated in Figure 6. We consider an axisymmetric model in cylindrical coordinates to reduce the complexity of the simulation. Consequently the model of the package is disc shaped. In this geometry, we model the full composite structure of the package including the copper lead frame and contacts, the silicon die, the epoxy glues and the plastic casing. Material properties of each of the component parts are listed in Table 2. The load is applied over a 1mm wide annular region on top of the package. The upward forces exerted by the pins are positioned under the contact on the outside edge of the bottom of the package and at the centre under the lead frame. We distribute the downward load between the inner and outer pins with a 1:5 ratio respectively to reflect the fact that there are more pins around the outside of the package. This is an approximation since the pins are not completely stiff and hence may distribute the load differently. The point at the base of the edge of the package is held fixed.

In Figure 7, we illustrate the deformation under loading of a cross-section of the package. Note that the scale of the displacements have been increased to accentuate the change in shape. We

38
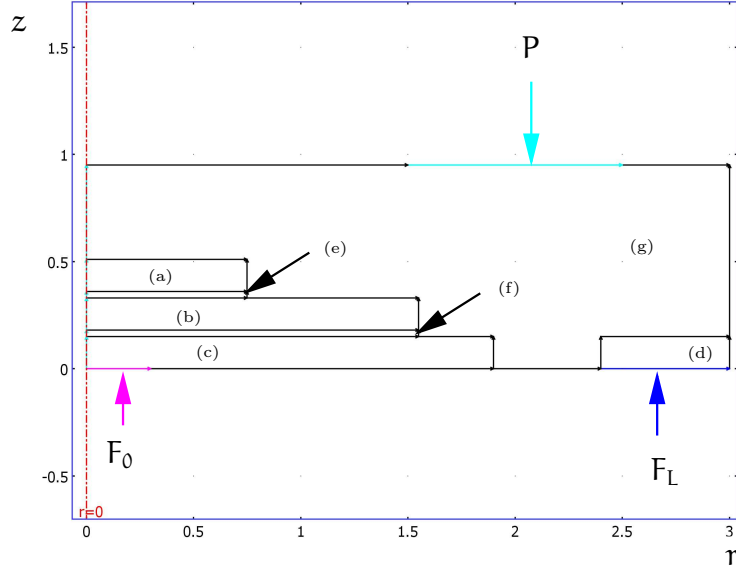
Figure 6: Cross-section of the numerical simulation set-up for the linear elasticity calculation in axisymmetric coordinates. The composite package is modelled, including: (a) top die, (b) bottom die, (c) lead frame, (d) contact, (e) and (f) epoxy glues, (g) plastic case. The applied load is labelled P and the reaction forces from the pins on the contacts and lead frame are labelled F_L and F_L respectively. These forces are distributed over the coloured regions.

observe that the maximum displacement (shaded in dark red) occurs where the downward force is applied and, due to the boundary conditions, there is no displacement at the bottom of the outer edge (shaded dark blue). The centre of the package ($r = 0$) is also displaced vertically since there is less support from the pins. Thus a slice through the full diameter of the package would resemble Figure 4(a), i.e a W–shape. Furthermore, if we reduce the load supported at the centre of the package, we find that the deformed package becomes concave, as in Figure 4(b).

The ϵ_{rr} strain field in the lead frame, top and bottom die are illustrated in Figure 8. We have omitted the strain field in the rest of the package since the circuitry lies in a thin layer on the surfaces of the two die, i.e. in the (r, θ) plane. Furthermore, the plastic casing and epoxy glues are much softer than the die and lead frame and consequently the magnitudes of their strains are much larger. Note that the strains on the top surfaces of the die where the electrical components are placed are much less on the top die than on the bottom. This accounts for the fact that the problems with the accuracy of the frequency of the oscillator circuit came to light after it was moved from the top die to the bottom die.

39

Young's Modulus	E, GPa
Lead frame (Cu)	127
Contacts (Cu)	127
Die (Si)	150
Epoxy Glue - bottom	3.1
Epoxy Glue - top	0.3
Plastic case	0.2

Table 2: Material properties used in linear elasticity simulation.
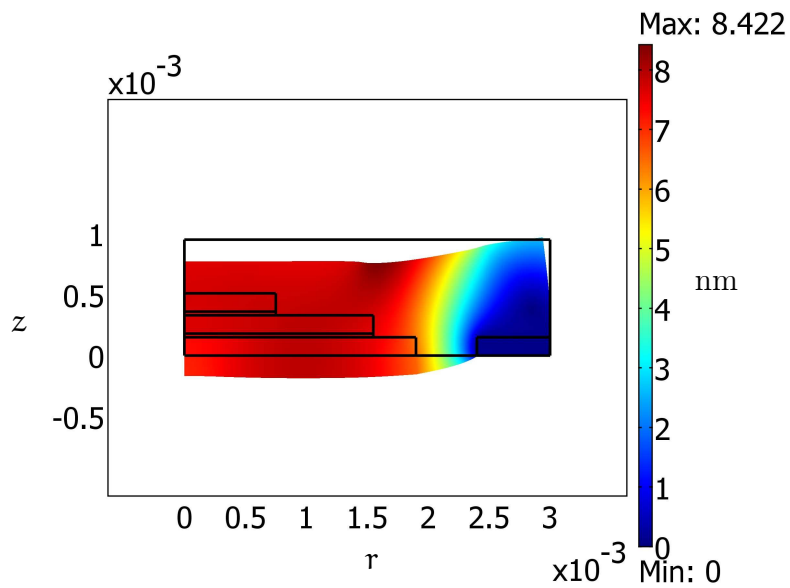
Figure 7: Deformation of the package under loading. The black out line illustrates the original position and the shaded region shows the subsequent deformation. The colour correspond to the magnitude of the total displacement. These have been greatly enhanced in this picture to illustrate the qualitative behaviour of the package.
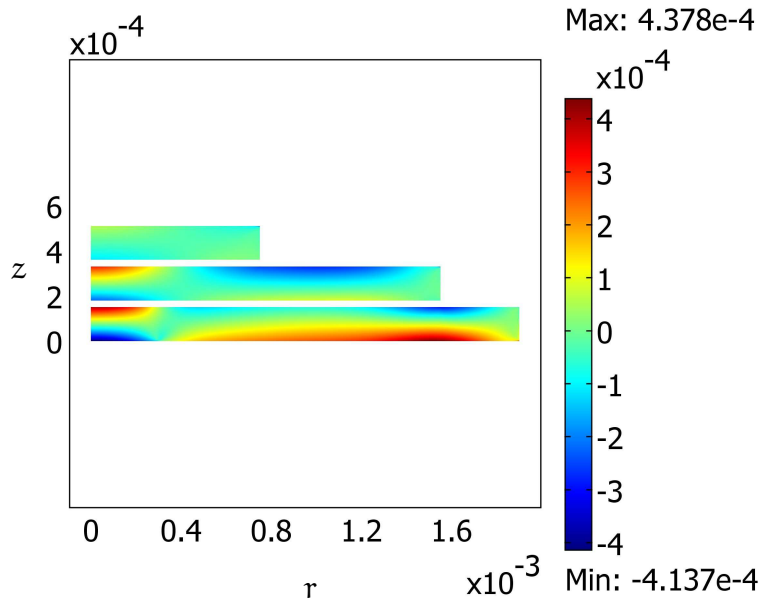
Figure 8: The coloured shading indicates the ϵ_{rr} strain field in the lead frame, top and bottom die. Note that the lead frame is stretched, however the bottom die is compressed.
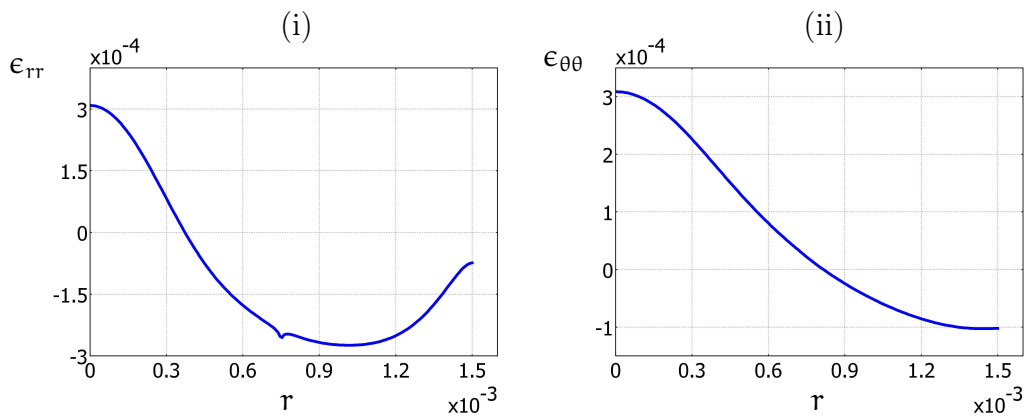
Figure 9: The strains ϵ_{rr} (a) and $\epsilon_{\theta\theta}$ (b) along the top surface of the bottom die in the r-direction.

41

In Figures 9(a) and (b) we plot the ϵ_{rr} and $\epsilon_{\theta\theta}$ strains respectively against r at the z–position corresponding to the top surface of the bottom die. The oscillator circuit lies in this plane, between the edge of the top die ($r = 0.75$) and the edge of the bottom die ($r = 1.5$). The magnitude of the strains there are large enough to account for the observed change in frequency due to the piezoresistive effect. Note that because of the W–shape of the package, there is a change in the sign of the strain. Furthermore, toward the outer edge of the package, the $\epsilon_{\theta\theta}$ strain is less than the ϵ_{rr} strain. Thus a qualitative feature of our simulation results is that an appropriate choice of position and orientation of the components of the oscillator circuit on the bottom die would minimise the strain they experience. We stress however that computing the strains within the package with enough precision to achieve this would require extending the geometry to three dimensions in rectangular coordinates (which requires far greater computational power) as well as a detailed knowledge of the components themselves.

5   Conclusion and Recommendations

This report investigates the possibility that inaccuracies in the frequency of an electronic oscillator measured under test conditions may be due to mechanical deformation of the chip containing the oscillator that occur during testing. We show that the most likely explanation is that the oscillator frequency is modified by the piezoresistive effect and estimate that the observed variations could be produced by tensile strains of the order of 10^{-4}. We carried out two elasticity calculations: a highly simplified calculation based on the beam equation and a second, considerably more sophisticated, treatment using finite element analysis. These simulations both demonstrated that strains the of the order of 10^{-4} in magnitude occur within the die, which explains the drift in oscillator frequency during test conditions.

From our simulations, we observe that the strain is largest directly underneath the nozzle that pushes down on the package and that the strains are significantly lower in the top die. Thus one might consider relocating the oscillator circuit or changing the shape of the nozzle that applies the downward force in order to reduce the strain in the package. Another possible solution could involve tuning the method in which the oscillator circuit is trimmed such that components which undergo lower values of strain are chosen preferentially.

Acknowledgements

Bibliography

[1] A.R. Hambley. *Electronics*. Prentice-Hall, second edition, 2000.

[2] Colin D. Simpson. *Industrial Electronics*. Prentice-Hall, first edition, 1996.

[3] L.D. Landau, E.M. Liftshitz, and L.P. Pitaevskii. *Electrodynamics of Continuous Media*. Butterworth-Heinemann, second edition, 1984.

[4] S. Middelhoek and S.A. Audet. *Silicon Sensors*. Academic Press Ltd., first edition, 1989.

[5] Yozo Kanda. Piezoresistance effect of silicon. *Sensor Actuat. A*, 28:83–91, 1991.

[6] Charles S. Smith. Piezoresistance effect in germanium and silicon. *Phys. Rev.*, 94(1):42–49, 1954.

[7] L.D. Landau and E.M. Liftshitz. *Theory of Elasticity*. Butterworth-Heinemann, third edition, 1986.

[8] COMSOL AB. *COMSOL Multiphysics Modeling Guide*. COMSOL Ltd, 3.4 edition, 2007.